



Trade Science Inc.

# Materials Science

An Indian Journal

Full Paper

MSAIJ, 8(11), 2012 [454-462]

## Microstructure stability of three carbides-strengthened cobalt-based alloys in the first times of thermal cycling

Patrice Berthod

Institut Jean Lamour (UMR 7198), Team 206 'Surface and Interface, Chemical Reactivity of Materials' University of Lorraine, F.S.T., B.P. 70239, 54506 Vandoeuvre-lès-Nancy, (FRANCE)

E-mail : Patrice.Berthod@univ-lorraine.fr

Received: 15<sup>th</sup> April, 2012 ; Accepted: 4<sup>th</sup> October, 2012

### ABSTRACT

The alloys for applications at high temperature may microstructurally evolve in service. This is notably the case of the volume fractions and of the morphologies of the carbides reinforcing the alloys issued from certain families, as the cobalt-based superalloys. If these phenomena are obvious after a long time spent at high temperature, they may start during the first hours of thermal cycling, with more or less consequences, this notably depending on the amount and the natures of the strengthening carbides. In this work, two types of carbides among the most used ones, were considered in a Co-30Cr alloy base: tantalum carbides and chromium carbides, either separately or present together. Four maximal temperatures were studied, between 1050 and 1250°C, for the 2 hours isothermal stage of the thermal cycle. After three cycles the microstructures of the alloys were analysed by SEM observations, DRX runs and image analysis measurements to characterize the microstructure evolution from the initial as-cast state. This evidenced a rapid evolution of both morphology and volume fraction of carbides which should continue during the following cycles, as shown by the great differences still remaining with the thermodynamic calculations performed for the stage temperatures.

© 2012 Trade Science Inc. - INDIA

### KEYWORDS

Cobalt alloys;  
Carbides;  
Thermal cycling;  
Microstructure stability;  
Thermodynamic calculations.

### INTRODUCTION

Among the refractory {hot corrosion + creep}-resistant metallic alloys which are commonly called "superalloys" there are the cast alloys based on cobalt and which are reinforced by carbides. The latter are the primary ones formed in the interdendritic spaces at the end of solidification, and the secondary ones appeared in the matrix, during special multi-stage heat treatment,

as homogeneously dispersed fine particles<sup>[1]</sup>. Although it concerns rather not many high temperature materials this family of superalloys remains still important for applications requiring high chromium amounts for the corrosion resistance against aggressive liquid substances as molten glass<sup>[2]</sup>.

During their use at high temperature the carbides strengthening the concerned cobalt alloys undergo morphological changes of long times, for example in simple

isothermal conditions, with problems of rarefaction<sup>[3]</sup> – in terms of decreasing surface fraction as well as of coalescence – and fragmentation<sup>[4]</sup>. But this can also occur when the alloy is subjected to variations of temperature, even for shorter values of cumulated times. If, in this field, the microstructure behaviour of cobalt alloys containing carbides is rather well known, the carbide evolution in conditions of thermal cycling needs to be deeper studied in the case of special kinetic conditions of temperature variations. This is precisely the aim of the present work to apply several { three cycles } – thermal tests to three different model alloys, and to compare the final microstructures to the initial ones, with interpretations helped by thermodynamic calculations.

## EXPERIMENTAL

Three chemical composition of alloys were considered in this work: Co (bal.)-30Cr-0.3C, Co (bal.)-30Cr-0.3C-4.5Ta and Co (bal.)-30Cr-0.6C-4.5Ta, all contents being expressed in weight percents. The choice of these compositions, based on previous works concerning this family of alloys, was governed by the wish of obtaining chromium carbides only (first alloy), tantalum carbides only (second alloy), or a mix of the two types of carbides (third alloy). These three alloys were elaborated by foundry under inert atmosphere, from initial charges composed of pure elements (Co, Cr and Ta: Alfa Aesar, purity higher than 99.9 wt.%; C: graphite). They were melted and solidified in the water-cooled copper crucible of a CELES high frequency induction furnace in an inert atmosphere composed of pure argon (300mbars). The three obtained ingots, all of about forty grams, were then cut to obtain a sample for the metallographic examination of the as-cast microstructure, and several parallelepipeds of about  $3 \times 5 \times 5 \text{ mm}^3$  for the thermal cycling tests.

The thermal cycling tests, performed in inert atmosphere, were composed of:

- a heating at  $10^\circ\text{C min}^{-1}$  from the ambient temperature to the targeted high temperature ( $T_{\text{stage}}$ ),
- an isothermal stage of 2 hours at  $T_{\text{stage}}$ ,
- a cooling at  $-10^\circ\text{C min}^{-1}$  down to room temperature, this being repeated three times.

The as-cast sample as well as the samples previously subjected to thermal cycling (these ones cut again

to reveal the core microstructure), were embedded in a cold resin mixture (manufacturer ESCIL: resin CY230 + hardener HY956) and polished with SiC papers from 240 to 1200 grit, with final polishing done using a textile disk containing  $1 \mu\text{m}$  alumina particles. The metallographic observations were done using a Field Emission Gun - Scanning Electron Microscopy (FEG-SEM: Hitachi S-4800), in the Back Scattered Electrons mode (BSE, 20kV). Several micrographs were taken at different magnifications between  $\times 250$  and  $\times 1000$ . These ones were exploited to illustrate the microstructures and to measure the surface fractions of the two types of carbides by image analysis (software Adobe Photoshop CS). X-Ray Diffraction runs were additionally performed to specify the natures of the carbides, using a Philips X'Pert Pro diffractometer (wavelength  $\text{Cu K}_\alpha$ : 1.5406 Angströms).

In order to interpret the microstructure evolution of the alloys thermodynamic calculations were performed using the Thermo-Calc version N software<sup>[5]</sup> and a database initially containing the descriptions of the Co-Cr-C system and its sub-systems<sup>[6-11]</sup> enriched by the description of the binary and ternary sub-systems Ta-C, Co-Ta, Cr-Ta and Co-Ta-C<sup>[12-15]</sup>. The natures and volume fractions of the phases stabilized at high temperature and still present after return to room temperature were thus compared to the natures and mass fractions converted in volume fractions given by the thermodynamic calculations performed for the chemical compositions of the alloys and the different temperatures of 2 hours - stage during the thermal cycling. For the conversion of the mass fractions into volume fractions the following volume masses were used<sup>[16]</sup>:  $8.9 \text{ g cm}^{-3}$  for the matrix,  $6.94 \text{ g cm}^{-3}$  for the  $\text{Cr}_7\text{C}_3$  carbides and  $14.5 \text{ g cm}^{-3}$  for the TaC carbides.

## RESULTS AND DISCUSSION

### As-cast microstructures of the alloys

Just after solidification and cooling the three alloys displays the microstructures presented in Figure 1 for the “Co3C” alloy (Co-30Cr-0.3C alloy), the “Co3CT” alloy (Co-30Cr-0.3C-4.5Ta) and the “Co6CT” alloy (Co-30Cr-0.6C-4.5Ta). In each case the main micrograph is a one taken at a magnification of  $\times 250$  to have

## Full Paper

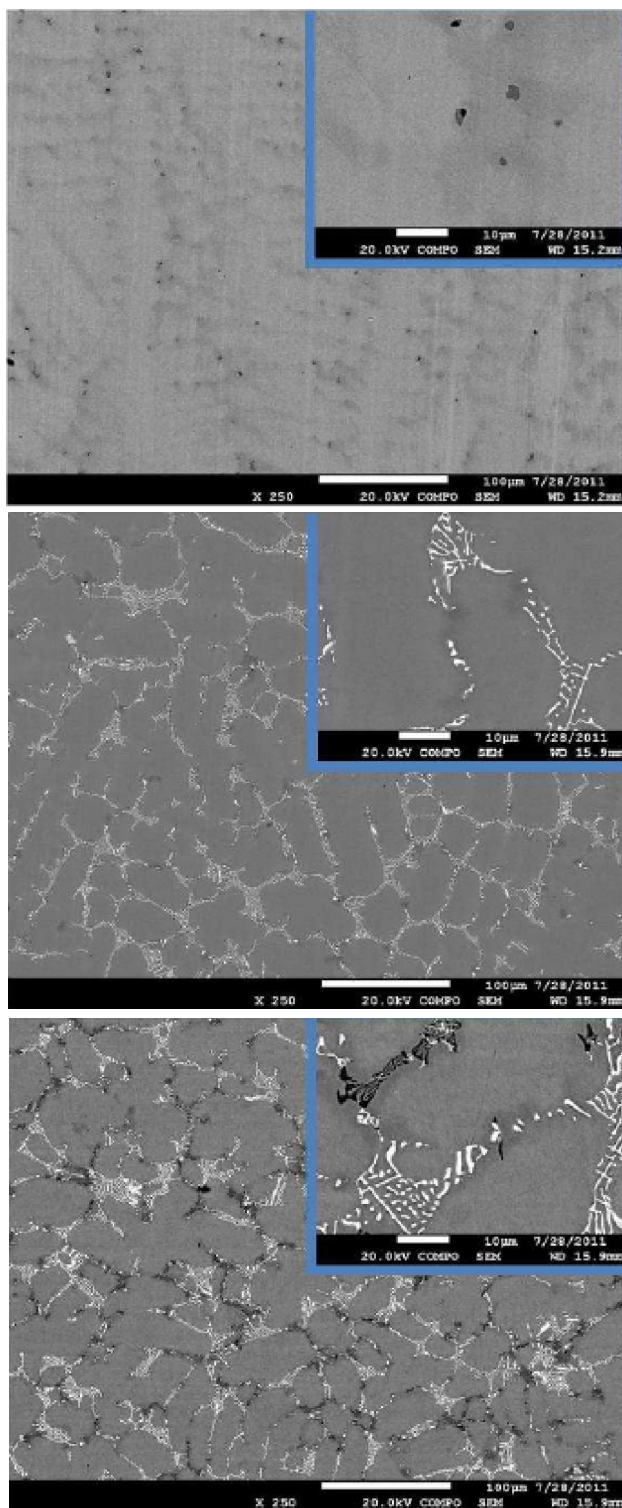


**Figure 1 :** The as-cast microstructures of the three alloys (Co3C: top, Co3CT: middle, and Co6CT: bottom); in all cases: pictures taken at  $\times 250$  (main picture) and  $\times 1000$  (inserted enlarged view)

a general view on the microstructure and the one inserted in the top-right corner is a more detailed view of the carbides' morphology (at  $\times 1000$ ).

The three alloys display a dendritic matrix and interdendritic carbides. Seemingly, in these micrographs obtained in Back Scattered Electrons mode, these carbides are exclusively chromium carbides (dark particles) in the Co3C alloy, exclusively tantalum carbides (white particles) in the Co3CT alloy. The Co6CT alloy seems containing both chromium carbides and tantalum carbides.

### Microstructures after the three cycles- thermal runs

By comparison with the as-cast microstructure illustrated in Figure 1 (top-left), the microstructural state of the Co3C alloy has significantly changed after thermal cycling, less for a stage temperature of  $1050^{\circ}\text{C}$  than for the two highest stage temperatures ( $1150$  and  $1200^{\circ}\text{C}$ ). Indeed, as evidenced by the micrographs presented in Figure 2, the initial chromium carbides have either diminished ( $1050^{\circ}\text{C}$ ) or almost disappeared ( $1150$  and  $1200^{\circ}\text{C}$ ). This is confirmed by the X-Ray Diffraction patterns which never really show peaks corresponding to the carbides since, in all cases, these ones are now inexistent or present in two small quantities to be detected. These XRD patterns show in addition that a part of austenite may still exist in the matrix (become essentially HCP) after the final cooling to room temperature (especially for  $T_{\text{stage}} = 1050^{\circ}\text{C}$ ).

As evidenced by the micrographs presented in Figure 3 the resistance of the carbides of the Co3CT alloy to the repeated exposure to high temperature is obviously much better for the TaC carbides since they are still present in great quantity after each thermal cycling test, although one can note that these quantities are at least a little lowered and that the carbides' integrity was affected, by comparison to the as-cast microstructure. More precisely it seems that the TaC carbides are present in slightly lower quantities and significantly more fragmented when the stage temperature was higher. Despite that the carbides (TaC) are much less numerous than in the carbides in the Co3C alloy, the XRD patterns do not systematically detect the presence of these carbides. Indeed, when present, the peaks revealing the presence of TaC carbides are rather small. Inversely the peaks corresponding to the matrix are of course here too more accentuated and they demonstrate here again that the matrix is generally partly aus-

tenitic (FCC) and partly hexagonal (HCP).

The same phenomena of quantity decrease and fragmentation increase of the TaC carbides, both enhanced by a higher stage temperature, are encountered for the Co6CT alloy (Figure 6). The chromium carbides are seemingly still present but less visible than in the as-cast microstructure. The XRD patterns better show here the presence of the TaC carbides, while additional peaks tend to reveal the presence of the other carbides but without allowing to really discriminate between the two probable chromium carbides type:  $M_7C_3$  or  $M_{23}C_6$ .

### Thermodynamic calculations

To help for the microstructure identification and for comparison purpose thermodynamic calculations were performed using the Thermo-Calc version N software. The results of these calculations, computed for the three or four stage temperatures, are presented in TABLE 1 for the Co3C alloy, TABLE 2 for the Co3CT alloy and in TABLE 3 for the Co6CT alloy.

One can see first that matrix may be austenitic at all

the stage temperatures and then that the thermal cycling involved at each cycle the change of its crystalline network from {HCP + FCC} (as revealed by XRD) to FCC and the inverse partial transformation at cooling. Concerning the carbides the thermal cycling may induce a change of nature of the chromium carbides, between their high temperature type ( $M_7C_3$ ) and their low temperature type ( $M_{23}C_6$ ), only in the case of  $T_{stage} = 1200$  and  $1250^\circ\text{C}$  for the Co3C alloy, and of  $T_{stage} = 1250^\circ\text{C}$  for the Co3CT alloy. But it was decided to experimentally try only 1050, 1150 and  $1200^\circ\text{C}$  for these two chromium carbides - containing alloys to remain far from the temperature of fusion start for these two alloys the refractoriness of which is known to be lowered by the presence of eutectic chromium carbides. Concerning the Co3CT alloy, cycling may induce disappearance at heating and possible re-precipitation at cooling. However, the rather long isothermal stage durations (even if they are of only 2 hours per cycle), in balance with the rather fast heating and cooling, may lead to the keeping of the high temperature types of

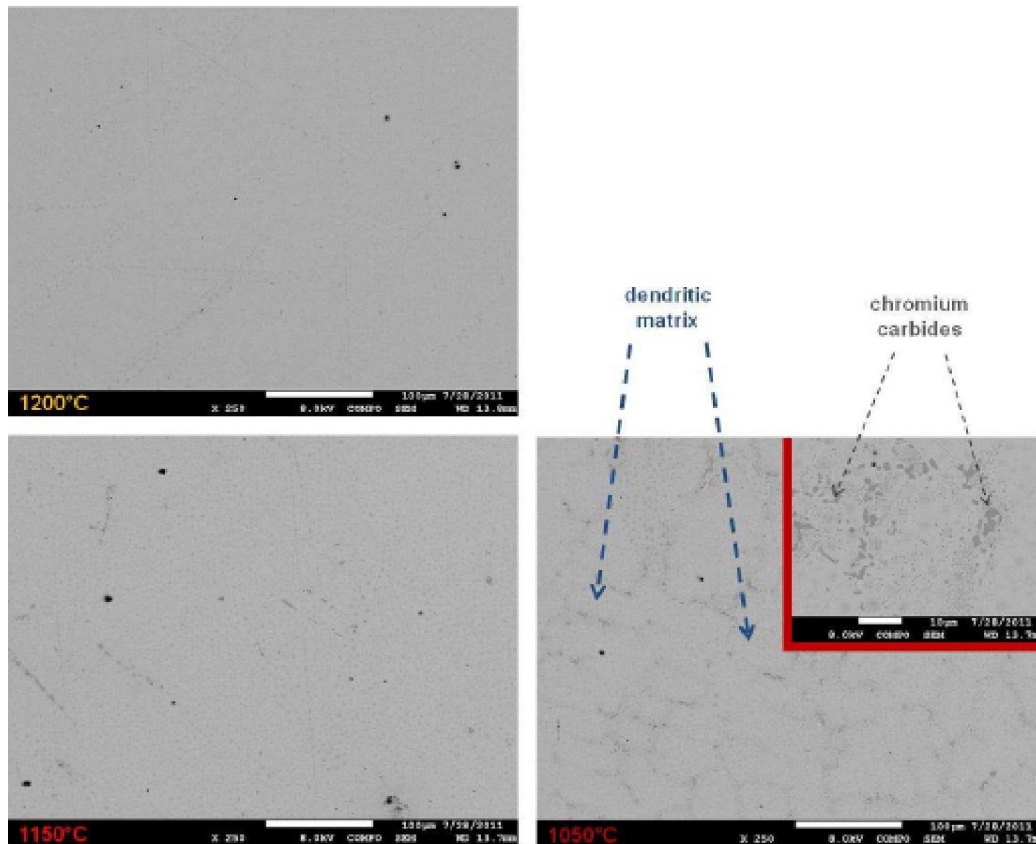
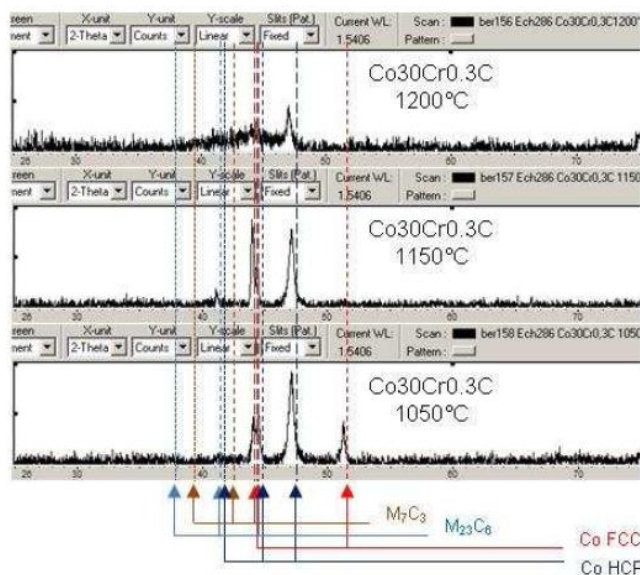


Figure 2: The microstructure of the Co3C alloy after thermal cycling; bottom right:  $3 \times 2\text{h}$  at  $1050^\circ\text{C}$ , bottom left:  $3 \times 2\text{h}$  at  $1150^\circ\text{C}$  and top left:  $3 \times 2\text{h}$  at  $1200^\circ\text{C}$ ; in all cases: pictures taken at  $\times 250$  (main picture) and  $\times 1000$  (inserted enlarged view)

## Full Paper



**Figure 3 :** XRD-aided identification of the matrix network and of the carbides' types for the Co3C alloy after thermal cycling; bottom: 3 × 2h at 1050°C, middle: 3 × 2h at 1150°C and top: 3 × 2h at 1200°C

carbides, in contrast with the metallic matrix which may transform faster during temperature changes (as proven

by the at least partial transformation in HCP evidenced by XRD).

### Measurement of the carbide surface fractions by image analysis

According to Thermo-Calc it also appears that the carbides, which should be of course present in greater quantities (when considered all together) if the carbon content is higher and if the concerned metal is a stronger carbide-former, would be present in lower quantities when the stage temperature is higher. This is in qualitatively good agreement with the metallographic observations. This can be more quantitatively studied by measuring the surface fractions of the carbides present in the alloys after thermal cycling. The results of image analysis are presented in TABLE 4, as well as the theoretic volume fractions calculated from the mass fractions issued from the thermodynamic calculations. It appears that, although there is one time a good agreement between real carbides surface fractions and calculated volume fractions (Co3CT at 1250°C) there is

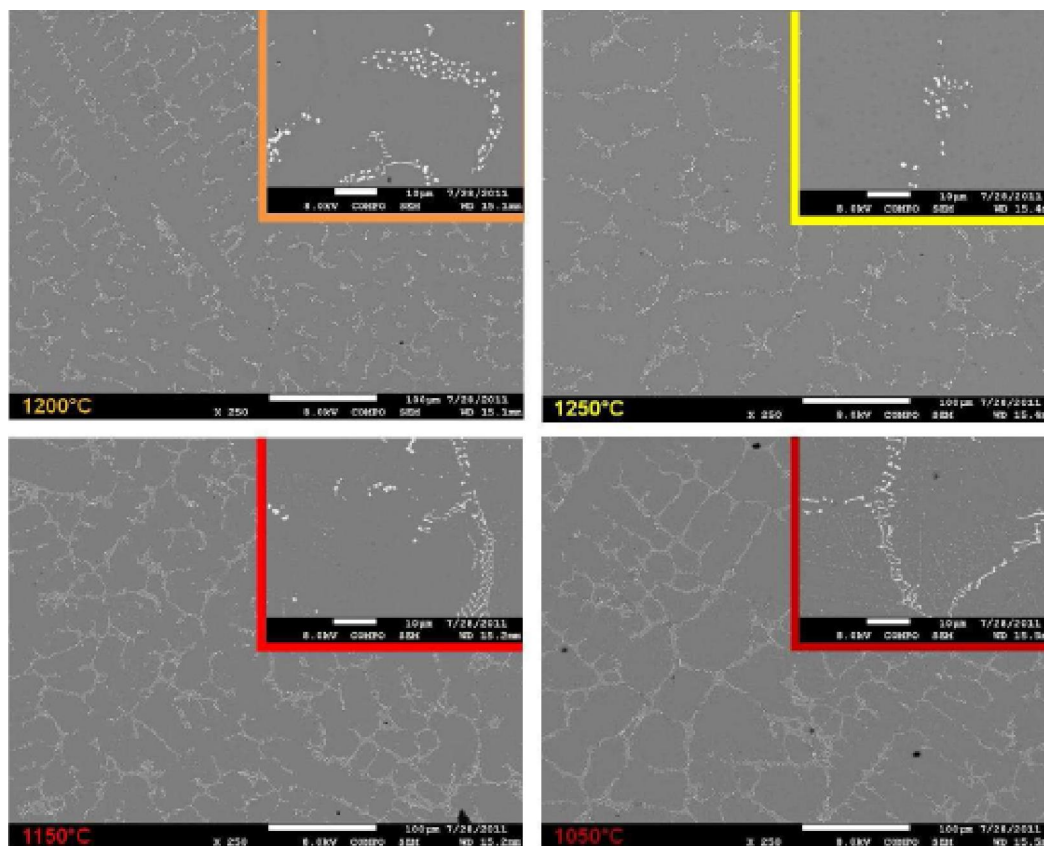


**Figure 4:** The microstructure of the Co3CT alloy after thermal cycling; bottom right: 3×2h at 1050°C, bottom left: 3×2h at 1150°C, top left: 3×2h at 1200°C and top right: 3×2h at 1250°C; in all cases: pictures taken at ×250 (main picture) and ×1000

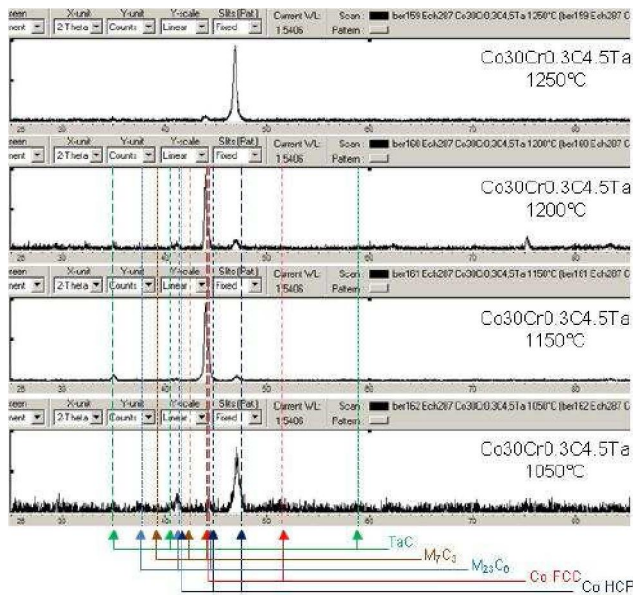


**Figure 5: XRD-aided identification of the matrix network and of the carbides' types for the Co3CT alloy after thermal cycling**

generally significant mismatches between the two sets of values: much less chromium carbides than calculated

in the Co3C alloy for all temperatures, much more tantalum carbides than calculated in the Co3CT alloy for all temperatures, and simultaneously much more tantalum carbides and much less chromium carbides than calculated in the Co6CT alloy also for all temperatures. It can also be noted that the alloys exposed to thermal cycling generally contain more chromium carbides and/or less tantalum carbides than in their as-cast conditions.

### General commentaries

Comparison with their point of departure (as-cast state) the alloy have significantly evolved microstructurally. In one case, alloy Co3C, the single type of carbide – chromium carbide – the as-cast microstructure was very poor of carbides and there was after thermal cycling that carbides had become visible (essentially for the two stage temperatures not too high). Since the thermodynamic calculations indicated higher values of volume fractions (after conversion of the mass fractions), one can think that the microstructure evolu-

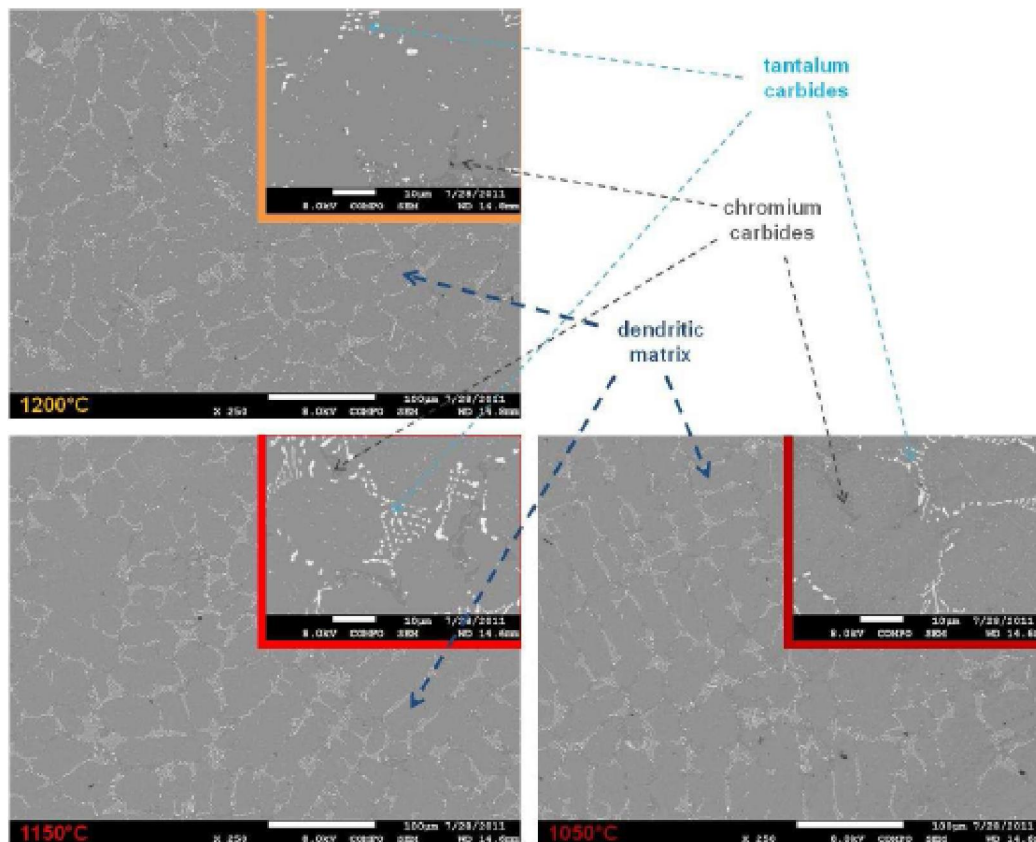


**Figure 6: The microstructure of the Co6CT alloy after thermal cycling; bottom right: 3×2h at 1050°C, bottom left: 3×2h at 1150°C and top left: 3×2h at 1200°C; in all cases: pictures taken at ×250 (main picture) and ×1000 (inserted enlarged view)**

## Full Paper

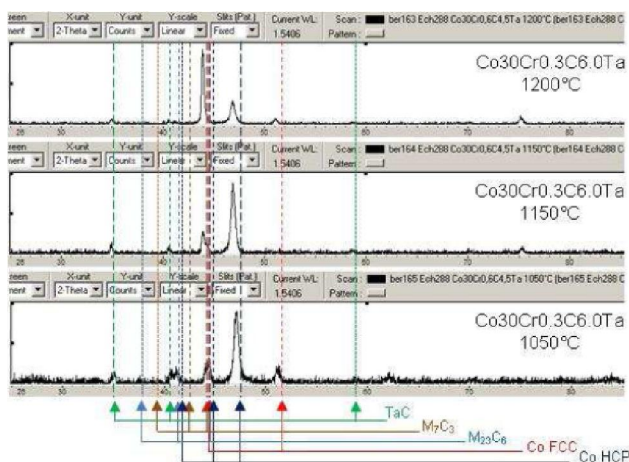


**Figure 7: XRD-aided identification of the matrix network and of the carbides' types for the Co6CT alloy after thermal cycling; bottom: 3 × 2h at 1050°C, middle: 3 × 2h at 1150°C and top: 3 × 2h at 1200°C**

tion should go on during additional cycles, with as result a progressive hardening of the alloy. This can be

initially due to a too rapid initial solidification which did not allow the precipitation of many carbides, this resulting for this ternary alloy in an as-cast microstructure still close to the high temperature solidification microstructure in terms of carbides fractions. The thermal cycling, by exposing the alloy to longer times at intermediate temperatures, allowed the carbides to grow and to go closer to the thermodynamic equilibrium at these temperatures. This evolution was obviously not finished since the obtained carbides fractions, after only three cycles containing a 2 hours-stage, were still rather far from the values of equilibrium.

For the Co3CT alloy, which contain almost only TaC carbides in the as-cast condition as well as after thermal cycling, the same as-cast low presence of tantalum carbides existed too, but this was less marked. However, during the three cycles of exposure to 1050°C the TaC volume fraction increases, to reach

**TABLE 1: Results of thermodynamic calculations for the Co3C alloy**

| $T_{stage}$ | Matrix: crystalline network |                                    | Carbide 1: nature |  | Carbide 2: nature |  |
|-------------|-----------------------------|------------------------------------|-------------------|--|-------------------|--|
|             | mass. %                     | chem. comp.(wt.%)                  | mass. %           | chem. comp.(wt.%)  | mass. %           | chem. comp.(wt.%)  |
| 1250°C      | 98.22                       | FCC<br>71.83Co - 29.03Cr<br>0.143C | 1.78              | M <sub>7</sub> C <sub>3</sub><br>83.59Cr - 8.93C<br>7.48Co | /                 | /  |
| 1200°C      | 97.91                       | FCC<br>71.04Co - 28.85Cr<br>0.115C | 2.10              | M <sub>7</sub> C <sub>3</sub><br>83.90Cr - 8.93C<br>7.17Co | /                 | /  |
| 1150°C      | 96.20                       | FCC<br>71.70Co - 28.20Cr<br>0.092C | /                 | /  | 3.81              | M <sub>23</sub> C <sub>6</sub><br>75.43Cr - 19.02Co<br>5.56C   |
| 1050°C      | 95.45                       | FCC<br>72.17Co - 27.78Cr<br>0.049C | /                 | /  | 4.55              | M <sub>23</sub> C <sub>6</sub><br>76.46Cr - 17.97Co<br>- 5.56C |

**TABLE 2: Results of thermodynamic calculations for the Co3CT alloy**

| $T_{stage}$ | Matrix: crystalline network |   | Carbide 1: nature |  | Carbide 2: nature |  |
|-------------|-----------------------------|---|-------------------|--|-------------------|--|
|             | mass. %                     | chem. comp.(wt.%)                           | mass. %           | chem. comp.(wt.%)                          | mass. %           | chem. comp.(wt.%)  |
| 1250°C      | 96.41                       | FCC<br>67.63Co - 31.11Cr<br>1.19Ta - 0.080C | 3.59              | TaC<br>93.47Ta - 6.22C<br>0.29Cr - 0.02Co  | /                 | /  |
| 1200°C      | 96.22                       | FCC<br>67.76Co - 31.17Cr<br>1.00Ta - 0.067C | 3.79              | TaC<br>93.50Ta - 6.22C<br>0.27Cr - 0.015Co | /                 | /  |
| 1150°C      | 96.04                       | FCC<br>67.89Co - 31.23Cr<br>0.83Ta - 0.06C  | 3.96              | TaC<br>93.52Ta - 6.22C<br>0.24C - 0.01Co   | /                 | /  |
| 1050°C      | 95.71                       | FCC<br>68.11Co - 31.28Cr<br>0.58Ta - 0.035C | 4.22              | TaC<br>93.58Ta - 6.23C<br>0.19Cr - 0.01Co  | 7.16              | M <sub>23</sub> C <sub>6</sub><br>79.10Cr - 15.32Co<br>5.58C - 0Ta |

TABLE 3: Results of thermodynamic calculations for the Co6CT alloy

| $T_{\text{stage}}$ | Matrix: crystalline network |   | Carbide 1: nature |   | Carbide 2: nature |   |
|--------------------|-----------------------------|---|-------------------|---|-------------------|---|
|                    | mass. %                     | chem. comp.(wt.%)                           | mass. %           | chem. comp.(wt.%)                         | mass. %           | chem. comp.(wt.%)                               |
| 1250°C             | 93.50                       | FCC<br>69.23Co – 29.85Cr<br>0.79Ta – 0.14C  | 4.04              | TaC<br>93.21Ta – 6.27C<br>0.49Cr – 0.03Co | 2.46              | $M_7C_3$<br>84.16Cr – 8.93C<br>6.90Co – 0Ta     |
| 1200°C             | 91.56                       | FCC<br>70.01Co – 29.17Cr<br>0.71Ta – 0.11C  | 4.13              | TaC<br>93.27Ta – 6.27C<br>0.44Cr – 0.03Co | 4.31              | $M_{23}C_6$<br>75.94Cr – 18.50Co<br>5.56C – 0Ta |
| 1150°C             | 91.10                       | FCC<br>70.30Co – 28.95Cr<br>0.66Ta – 0.08C  | 4.17              | TaC<br>93.36Ta – 6.26C<br>0.36Cr – 0.02Co | 4.72              | $M_{23}C_6$<br>76.38Cr – 18.06Co<br>5.56C – 0Ta |
| 1050°C             | 90.46                       | FCC<br>70.75Co – 28.63Cr<br>0.57Ta – 0.044C | 4.26              | TaC<br>93.51Ta – 6.24C<br>0.24Cr – 0.01Co | 5.29              | $M_{23}C_6$<br>77.39Cr – 17.03Co<br>5.57C – 0Ta |

TABLE 4: Surface fractions of carbides measured by image analysis and comparison with the volume fractions deduced from the mass fractions issued from the thermodynamic calculations

| $T_{\text{stage}}$ | Image analysis<br>/ Th. Calc | Co3C |             | Co3CT       |             | Co6CT       |             |
|--------------------|------------------------------|------|-------------|-------------|-------------|-------------|-------------|
|                    |                              | TaC  | $Cr_xC_y$   | TaC         | $Cr_xC_y$   | TaC         | $Cr_xC_y$   |
| 1250°C             | Im. Anal.                    | /    | /           | 1.91 ± 0.35 | 0.02 ± 0.01 | /           | /           |
|                    | Th. Calc                     | /    | /           | 2.23        | 0           | /           | /           |
| 1200°C             | Im. Anal.                    | /    | 0.42 ± 0.06 | 2.77 ± 0.27 | 0.03 ± 0.01 | 4.71 ± 1.51 | 1.66 ± 0.60 |
|                    | Th. Calc                     | /    | 2.68        | 2.36        | 0           | 2.54        | 5.55        |
| 1150°C             | Im. Anal.                    | /    | 0.92 ± 0.23 | 2.67 ± 0.38 | 0.02 ± 0.01 | 4.88 ± 0.72 | 2.51 ± 1.12 |
|                    | Th. Calc                     | /    | 4.83        | 2.47        | 0           | 2.57        | 6.07        |
| 1050°C             | Im. Anal.                    | /    | 2.54 ± 1.08 | 5.53 ± 0.99 | 0.23 ± 0.10 | 4.74 ± 0.83 | 3.05 ± 1.28 |
|                    | Th. Calc                     | /    | 5.76        | 2.63        | 0.09        | 2.62        | 6.79        |
| As-cast            | Im. Anal.                    | /    | 0.32 ± 0.11 | 3.86 ± 0.54 | 0.01 ± 0.01 | 4.18 ± 0.89 | 1.53 ± 0.28 |

higher volume fraction than predicted by Thermo-Calc. For the three highest stage temperatures, the TaC fractions obtained were in contrast lower than in the as-cast condition but higher again than the predicted ones. This can be explained by the fact that the tantalum atoms had maybe severely segregated towards the last zones to solidify and then promoted an initial formation of TaC carbides in these interdendritic spaces higher than predicted by thermodynamic calculations, later followed by an achievement of this interdendritic TaC precipitation during the stages at 1050°C. In contrast, the stage at temperature 100°C higher and more favoured fragmentation of the initial carbides (driving force: the interfacial energy reduction) and a smoothing of the segregation during solidification by inverse diffusion of the Ta atoms, leading to a better chemical homogeneity. The progress of carbide precipitation, of both TaC and chromium carbides, obviously also occurred for the super-

saturated matrix part surrounding the interdendritic spaces of the Co6CT alloy, with as result more tantalum carbides and more chromium carbides than in the as-cast condition. However, probably because a more difficult inverse diffusion of the big Ta atoms from outside to inside the matrix dendrites, by comparison with the smaller Cr atoms, the TaC carbides tend to be drastically more present and the chromium carbides less present, than indicated by Thermo-Calc.

## CONCLUSIONS

The first cycles – even short in time – of the cycling temperature evolution may lead to important microstructure evolutions of carbides-strengthened cobalt-based alloys, as demonstrated here with simple ternary and quaternary alloys. In these model alloys, the metallurgical instability of the microstructures resulting initially from

## Full Paper

rather fast solidification and solid state cooling, rapidly occurs, with as consequences, for the studied alloys, a probable strengthening effect (more carbides). However this may also induce problems as an initial mechanical deterioration of the alloys which are maybe not strengthened enough in the first hours of service, possible geometrical instabilities ... It appears to be better to stabilize the microstructures of the alloys by convenient heat-treatment after solidification (as usually done) to avoid such initial microstructure evolution, and then potential problems, before using the pieces in thermal cycling.

### ACKNOWLEDGEMENTS

The author wishes to thank Lionel Aranda and Thierry Schweitzer for their technical help, Pascal Villeger for the XRD experiments, and Ludovic Mouton (Common Service of Electron Microprobe and Microanalysis of the Faculty of Science and Technologies of the University of Lorraine) for the FEG - SEM examinations.

### REFERENCES

- [1] M.J.Donachie, S.J.Donachie; 'Superalloys: A technical guide', ASM International, Materials Park, **2**, (2002).
- [2] J.L.Bernard, C.Liébaud, P.Berthod, S.Michon; Patent FR 2862662 A1.
- [3] P.Berthod, S.Michon, L.Aranda, S.Mathieu, J.C.Gachon; Calphad, **27**, 353 (2003).
- [4] P.Berthod, C.Heil, L.Aranda; J.Alloys Compounds, **504**, 243 (2010).
- [5] Thermo-calc version n: 'Foundation for computational thermodynamics' Stockholm, Sweden, Copyright, (1993,2000).
- [6] A.Fernandez Guillermet; Int.J.Thermophys., **8**, 481 (1987).
- [7] J.O.Andersson; Int.J.Thermophys., **6**, 411 (1985).
- [8] P.Gustafson; Carbon, **24**, 169 (1986).
- [9] A.Fernandez Guillermet; Z.Metallkde, **78**, 700 (1987).
- [10] J.O.Andersson; Calphad, **11**, 271 (1987).
- [11] A.Fernandez Guillermet; Z.Metallkde., **79**, 317 (1988).
- [12] K.Frisk, A.Fernandez Guillermet; J.Alloys Compounds, **238**, 167 (1996).
- [13] Z.K.Liu, Y.Austin Chang; Calphad, **23**, 339 (1999).
- [14] N.Dupin, I.Ansara; J.Phase Equilibria, **14**, 451 (1993).
- [15] L.Dumitrescu, M.Ekroth, B.Jansson; Metall.Mater. Trans.A., **32A**, 2167 (2001).
- [16] Handbook of Chemistry and Physics, **57**, (1977).
- [1] M.J.Donachie, S.J.Donachie; 'Superalloys: A technical guide', ASM International, Materials